

ATTENUATION OF INTENSITY FOR THE 1887 NORTHERN SONORA, MEXICO EARTHQUAKE

BY MARC L. SBAR* AND SUSAN M. DUBOIS

ABSTRACT

Contouring the intensity data for the northern Sonora earthquake of 1887 yields an area of perceptibility defined by the MM III isoseismal that is greatly elongated to the southeast of the epicenter along the Sierra Madre Occidental. North of the epicenter, the isoseismals are compressed due to the change in crustal structure between the Colorado Plateau and the southern Basin and Range province. The higher intensity isoseismals are more symmetric, although local structure strongly influences individual intensity values. To evaluate the attenuation of intensity with distance, three regression curves are calculated as below

$$\text{All data: } I = 12.0 + 3.2 - 0.0015 R - 1.5 \ln(R)$$

$$\text{25-500 km: } I = 12.0 + 0.69 - 0.0069 R - 0.82 \ln(R)$$

$$\text{Iseismal: } I = 12.0 + 8.1 - 0.0031 R - 2.3 \ln(R)$$

where R is the epicentral distance in kilometers. The "All data" curve is derived from a regression computed using all 171 intensity values. The "25-500 km" curve eliminates the near and far points, and the "Iseismal" curve is a regression on the average radii of the area enclosed by each isoseismal contour. The latter two curves are similar to curves for the Western United States as a whole (Anderson, 1978) or the Cordilleran curve of Howell and Schultz (1975) for intensities less than or equal to MM X. The curve for "All data" indicates less attenuation at lower isoseismals than the other two 1887 regressions and falls between the Cordilleran and Eastern United States models of Howell and Schultz.

INTRODUCTION

The northern Sonora earthquake of 3 May 1887 is one of the largest, historic, normal faulting earthquakes in North America. Natali and Sbar (1982) calculated a seismic moment for this event of 1.27×10^{27} dyne-cm which is equivalent to a surface-wave magnitude of 7.4 (Hanks and Kanamori, 1979). The fault scarp resulting from this earthquake is clearly exposed on the east side of the San Bernardino Valley of northern Sonora just southeast of Douglas, Arizona. It extends in a north-south direction from near the Arizona border for a distance of 76 km to the south (Herd and McMasters, 1982). The maximum displacement is 4.5 to 5.1 m, and there is evidence for previous ruptures on this fault (Pitaycachi fault) with a recurrence interval of about 10^5 yr (Bull *et al.*, 1981; Pearthree *et al.*, 1983).

The recent seismic record and microearthquake studies in the summers of 1978 and 1979 by Natali and Sbar (1982) indicate that the fault is still the center of relatively high activity for this region. The current sense of motion determined from a composite fault plane solution of the microearthquakes is normal faulting on a steeply dipping plane striking approximately north-south. The west side is down, consistent with present topography and observed fault offsets.

The northern Sonora earthquake appears to be an isolated event in that it is not

* Present address: Sohio Petroleum Company, 1 Lincoln Center, Suite 1200, 5400 LBJ Freeway, Dallas, Texas 75240.

clearly part of an identified seismic or recognized contemporary tectonic trend. The Rio Grande Rift System is about 200 km east of the San Bernardino Valley, and the two have many similar characteristics (e.g., high heat flow, recent volcanism, a rift-like appearance with a relatively deep valley floor surrounded by high mountains). Seager and Morgan (1979) suggest that these similarities are indicative of a similar causative mechanism. Geomorphic work by Pearthree *et al.* (1983) identifies a north-south trending zone of relatively high activity involving a number of faults along the Arizona-New Mexico border in the southern part of both states, which extends southward into Sonora. They postulate that a period of quiescence between 6 and 3 m.y.b.p. existed after the Basin and Range deformation. This period was followed by increased activity post 3 m.y.b.p., which is continuing to the present. This north-south zone may continue south of the Pitaycachi fault for another 400 km based on the existence of a long straight valley with a fault mapped along its east side (de Cserna *et al.*, 1961).

The northern Sonora earthquake of 1887 caused widespread damage to property, 51 deaths, and many more injuries even though the region was sparsely populated. A significant region of liquefaction was reported up to 100 km from the fault. Landslides were observed to even larger distances (DuBois and Smith, 1980). Because the rupture length for this event is as great as the surface expression of any of the faults observed in southeastern Arizona and southwestern New Mexico (Pearthree *et al.*, 1983) and is larger than any other normal faulting earthquake known (Herd and McMasters, 1982) the 1887 earthquake may be regarded as the maximum possible earthquake in this region. As such, it warrants further study.

The spatial variation and the attenuation of intensity for the 1887 earthquake are the focus of this discussion. DuBois and Smith (1980) documented the individual felt reports for this earthquake from primary sources such as newspaper accounts, diaries and government documents, and assigned Modified Mercalli intensity values to each locality. These ratings provide the data base for the present analysis. In the following sections, the selection of intensity values to the reports are discussed. These values are then plotted and contoured producing the traditional isoseismal map. Finally, the data are then used to provide an estimate of the attenuation of intensity with distance, based first on the individual reports as suggested by Bollinger (1977) and second on the average epicentral distance of an isoseismal as is more commonly done.

ASSIGNMENT OF INTENSITY VALUES

The compilation of DuBois and Smith (1980) contains 214 localities at which intensity could be assigned. Because of the inadequacy of the old maps and possible name changes, coordinates of many towns and ranches were unable to be located, and only 171 entries are incorporated in the present analysis. These data are listed in the Appendix at the end of this manuscript. DuBois and Smith (1980) used the Modified Mercalli scale as listed by Richter (1958) and modified by Brazee (1979) for the intensity estimates. The modifications by Brazee attempt to classify the individual elements of the scale more rigorously by evaluating how each element varies with distance and epicentral intensity. Some significant changes between the traditional Modified Mercalli scale and Brazee's modified version were thus incorporated in the assignments of DuBois and Smith. In addition, the intensity value assigned to each locality (for which there may be one or many sources) was independently evaluated by Marc Sbar of the University of Arizona and Ruth Simon

of Woodward-Clyde Consultants. The final value was either the one selected in two of the three evaluations or the average of the three.

In general, the problems faced in the assigning intensities were sparsity or inconsistency of data and the inadequacy of the Modified Mercalli scale at large intensity values. At some localities only sketchy and divergent reports were available. DuBois and Smith assign a range of intensities to these sites. Brazee (1979) notes that there are few data at the upper end of the intensity scale from which the statistical reliability of the individual elements can be established. A blurring of these elements is also apparent in the DuBois and Smith compilation, leading to the assignment of a range of intensities to a site rather than a single value. One other notable problem with the Modified Mercalli scale as applied to this earthquake is the use of building damage as an indicator of intensity. Because the area was sparsely populated in 1887 and detailed accounts of building damage, building material and construction, etc., were not uniformly available throughout the area, ratings of damage to structures were difficult to assign with confidence. The intensity level MM XII was assigned to those areas in which clear evidence of surface faulting and severe ground failure exists. Surface faulting in firm rock is one element of the MM XII classification by Brazee (1979). "Firm rock" was not observed along the fault scarp, although it outcrops near the fault on the upthrown side.

Because liquefaction and landslides both occur over a wide range of intensity levels, these effects were not always diagnostic. They might be primarily dependent on the presence of a shallow water table and particular soil type, or in the case of landslides the grade of the slope and weathered state of the bedrock. It is possible that high values assigned to these reports may bias the contouring. In situations where a range of intensities was assigned to a site by DuBois and Smith, the average value was taken using $\frac{1}{2}$ units for the purpose of this attenuation analysis.

ISOSEISMAL PATTERN

The contouring of intensity values to produce Figure 1 is based on the most commonly observed values as suggested by Richter (1958). Because the data are sparse, each intensity level could not be individually contoured. In the immediate vicinity of the fault the isoseismals appear to be controlled by the San Bernardino Valley and the fault itself, since they are elongated parallel to these features. The valley and the fault both trend north-south. The north-south elongation of isoseismals is accentuated in the detailed contouring of the epicentral region of DuBois and Smith. The isoseismals of Figure 1 have been smoothed to show the overall pattern. The MM V-VI and VII isoseismals are roughly symmetric, while the MM VIII, IX, and XI-XII isoseismals are slightly elongated northwest-southeast, and the MM III isoseismal is greatly elongated to the southeast. The latter contour is based on a sufficient number of points to permit confidence in its shape. The MM III isoseismal appears to be primarily controlled by the structure of the Sierra Madre Occidental, which strikes southeast from the epicentral region. This isoseismal, however, is compressed in the northern part of the felt area near the boundary of the Colorado Plateau with the Basin and Range province. The other isoseismals are likewise influenced by the smaller scale basins and ranges of the southern Basin and Range. Based on the analysis of the attenuation of intensity in the mid-continent region by Nuttli (1973), the variations in intensity are assumed to be primarily due to the propagation of 3 to 6-sec period surface waves. Since the

propagation of surface waves is strongly affected by structures with size comparable to their wavelengths (11 to 22 km), they and the isoseismal pattern will be controlled by dramatic crustal velocity changes such as those found in the transition between the Basin and Range and the Colorado Plateau, and also between individual basins and ranges. Surface waves and the isoseismal pattern will also be influenced by the

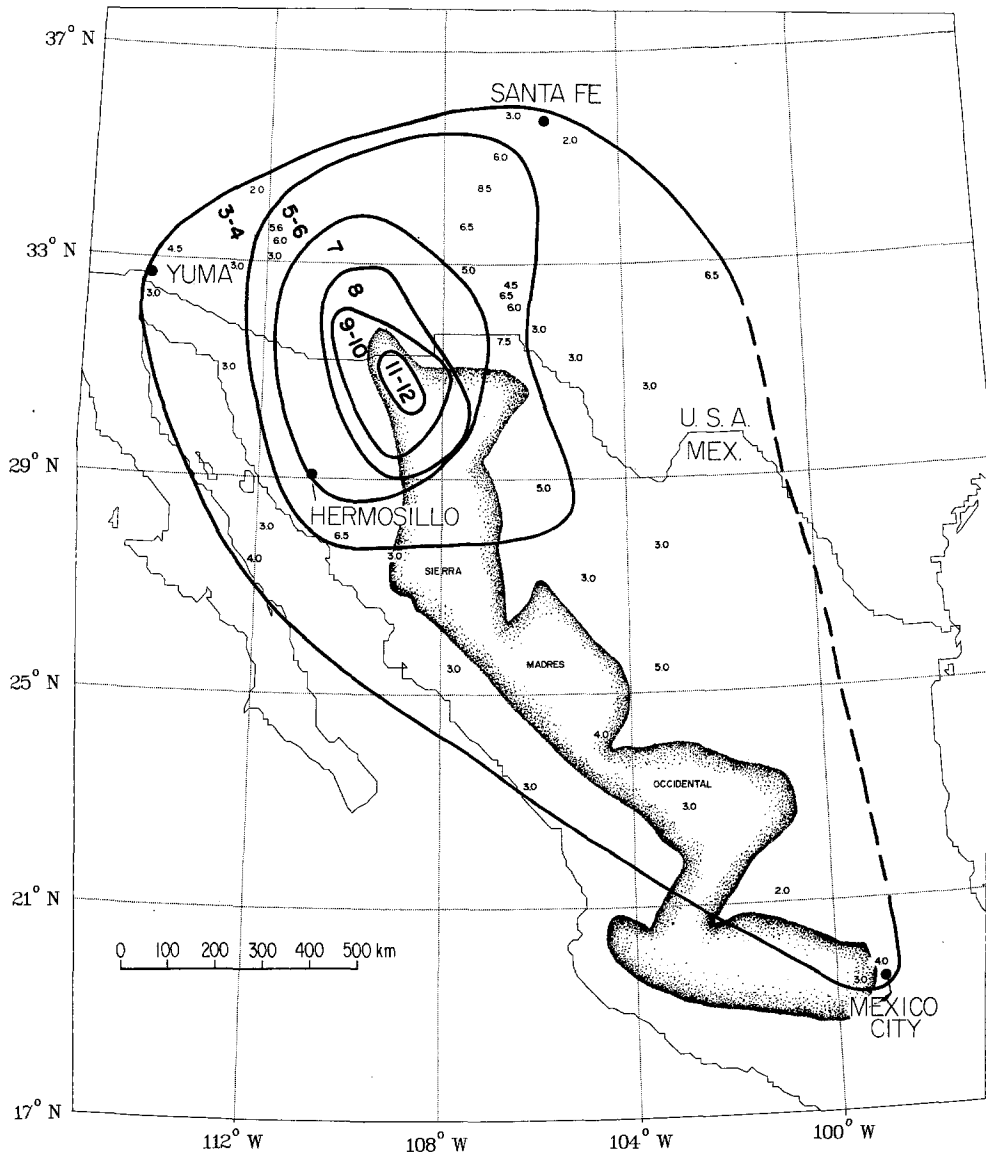


FIG. 1. Isoseismal contours based on 171 individual intensity values for the 1887 northern Sonora earthquake. In some cases, two intensity levels are grouped to permit contouring. The dashed isoseismal indicates insufficient data to define that part of the contour.

apparently uniform velocity structure and low attenuation of the Sierra Madre Occidental.

ATTENUATION

The attenuation of intensity with distance can be measured in several ways. Most commonly, an average distance from the epicenter to a particular isoseismal contour

is determined, and a regression is performed using these average values for analysis of intensity versus distance. If individual intensity values are available a regression on these can also be done using the distance from the epicenter to each site. The latter method is preferable, since there is less bias involved and confidence limits for the regression line are a better measure of the scatter in the individual data.

The 1887 northern Sonora earthquake occurred in an area for which no other reasonably complete isoseismal maps exist. It is necessary, therefore to base an attenuation analysis on data from this single event. For comparison, the regression computed using the northern Sonora data is plotted with other curves for the United States.

The regression is done using equation (1).

$$I = I_0 + a - bR - c \ln(R). \tag{1}$$

TABLE 1
REGRESSION COEFFICIENTS FOR EQUATION (1)

Description	No.*	<i>a</i>	<i>b</i>	<i>c</i>	<i>σI</i> †
Northern Sonora					
All	171	3.24	0.00150	1.54	1.52
25-500 km	140	0.693	0.00691	0.817	1.46
Isoseismals	1	8.14	0.00310	2.27	0.29
Howell and Schultz (1975)					
Eastern United States	5	3.28	0.0029	0.989	0.64
Cordillera	10	1.80	0.0090	0.628	0.61
San Andreas	10	0.87	0.0186	0.422	0.64
Anderson (1978)					
Western United States	—	3.2	0.00633	1.17	—
Gupta and Nuttli (1976)					
Central United States	2	3.7	0.0011	1.17	—
Bollinger (1977)					
Southeastern United States	780	2.87	0.00052	1.25	1.2

* The first two Northern Sonora values and Southeastern United States indicate the number of points. The other values are the number of earthquakes.

† rms standard deviation in intensity or isoseismals.

For all computations, I_0 is 12 R is the epicentral distance in kilometers, and the coefficients a , b , and c are given in Table 1 for the various cases, which are plotted in Figures 2 through 7. The epicentral distance is taken from the site of greatest displacement along the fault. As a result of this assumption, points at the ends of the fault scarp would not necessarily reflect the decrease of intensity with distance as would sites at the same distance, but perpendicular to the fault scarp. The fault extends for about 25 km to the north and 50 km to the south of the chosen epicenter.

Equation (1) is one of two expressions derived by Howell and Schultz (1975) that best fit the isoseismal data for various regions in the United States. Gupta and Nuttli (1976) and Bollinger (1977) use the same equation with logarithm to the base ten rather than natural logarithm. We use this equation for the purpose of comparison with these other analyses.

Figure 2 shows the individual data points on a semi-logarithmic plot, and a regression curve using equation (1) fit to all of the data.

The 95 per cent confidence limits indicate the confidence one would have in this curve as a predictor of the attenuation of intensity for another earthquake in the same area. That is, it is the 95 per cent probability that a different data set will produce an attenuation regression curve within the bounds noted, not the probability that an individual point will fall within these bounds. Standard deviations of the intensity residuals are also listed in Table 1. These values are a measure of the

1887 EARTHQUAKE

Regression - All Data

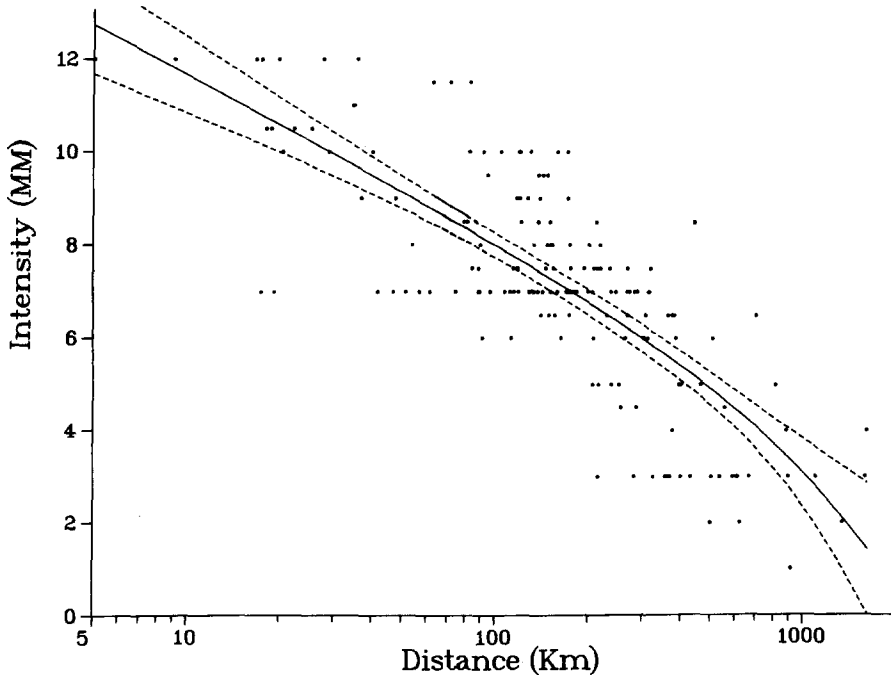


FIG. 2. All 171 intensity values versus distance on a semi-logarithmic plot. The solid curve is the regression on all data. The dashed curves are 95 per cent confidence limits on that curve.

scatter of the individual points about the curve. The curve of Figure 2 plots high at short epicentral distances because of MM XII points at distances of 30 km. The regression on all data shows lower attenuation than any of the following, as expected, because of the large distances to which the earthquake was felt along the axis of the Sierra Madre Occidental, which are eliminated or smoothed in Figures 3 and 4.

In order to develop a curve that may better predict intensity for the southern Basin and Range than the regression using the entire data set, a regression is

included that incorporates data within the range 25 to 500 km (Figure 3). The points near the epicenter are eliminated because some of them may actually lie along the fault. The points farthest from the epicenter were deleted because of the especially low attenuation along the strike of the Sierra Madre Occidental. This truncated data set yields a regression curve with more realistic intensity values at short epicentral distances and a smaller standard deviation.

To produce Figure 4, the areas circumscribed by each isoseismal contour are measured. The radius of a circle with the same area then becomes the average

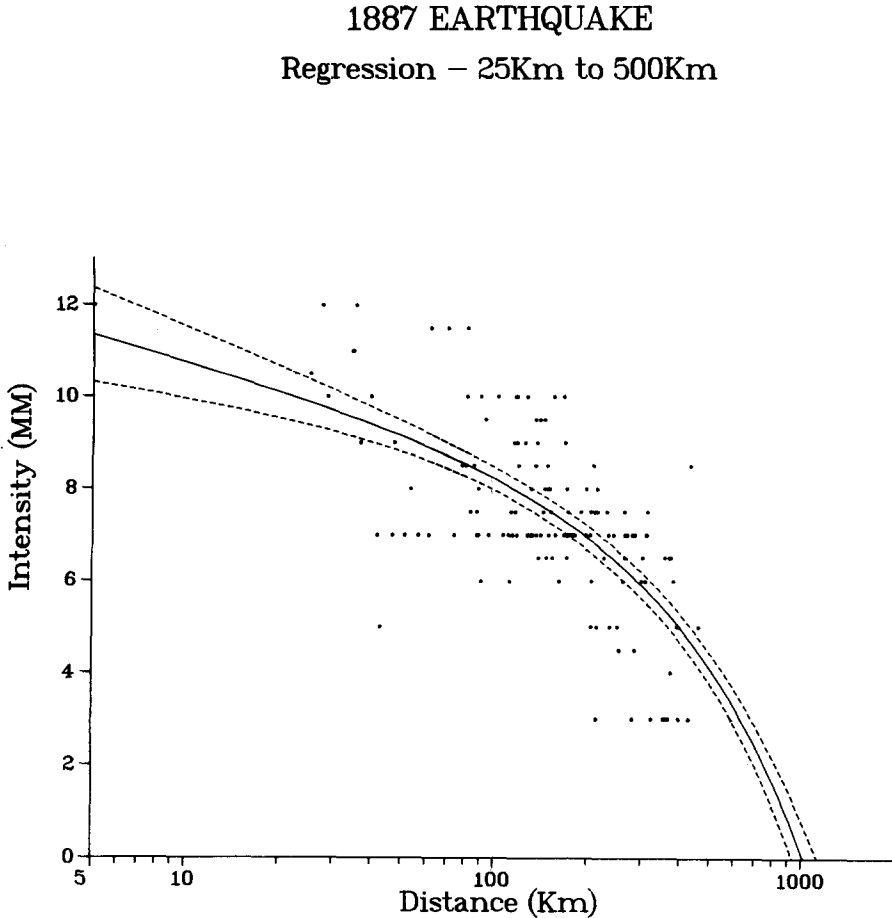


FIG. 3. Same as Figure 2, but the regression only includes data from distances 25 to 500 km from the epicenter.

epicentral distance for a particular intensity level (Table 2). These are plotted as triangles in Figure 4. Note that the 95 per cent confidence limits are much smaller in this case, since the data are greatly smoothed by the contouring process and the curve is tightly constrained by the data. Similar to the regression on all data, the isoseismal regression is high at short epicentral distances because of MM XII values to distances of 30 km. All of the data points are plotted in Figure 4 for comparison with the isoseismal averages.

COMPARISON WITH OTHER REGIONS

Figure 5 is a comparison of the regression curves in Figures 2 and 3 with that of Bollinger (1977) for the Charleston earthquake of 1886. All are based on an analysis of the individual site reports. The Bollinger curve uses data for distances greater than 50 km. As expected, the attenuation in the southern Basin and Range is greater than that in southeastern United States. The shape of the Bollinger curve and that for "all points" are quite similar primarily because of the low attenuation to the southeast of the northern Sonora epicenter.

1887 EARTHQUAKE Regression - Isoseismals

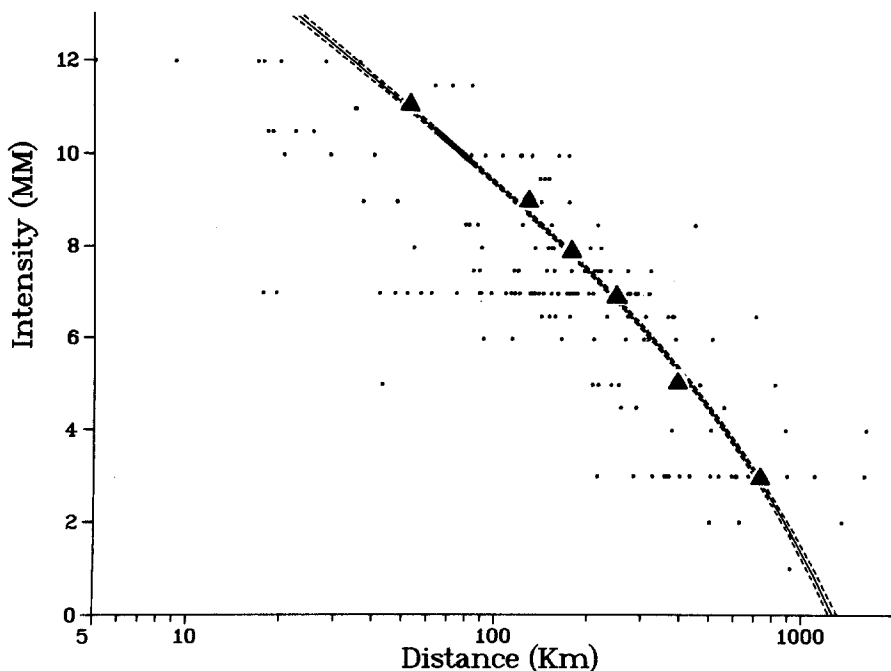


FIG. 4. Same as Figure 2 with all data points, but the regression is computed using the average isoseismals of Figure 1 as discussed in the text. The triangles are the isoseismal radii. Intensities greater than XII indicate the inadequacy of the regression at short distances and high intensities. All 171 data points are plotted for comparison.

The regression curves of Anderson (1978) for Western United States and Gupta and Nuttli (1976) for Central United States are based on isoseismals and are plotted with the three curves of Figures 2 to 4 and Figure 6. Gupta and Nuttli determined average distances for each isoseismal as described in Figure 4 above. Anderson computed similar isoseismal averages, but retained a measure of the anisotropy of the pattern in his standard deviations. The regression curve used by Anderson is not a best fit to his data, but is used only to compare his analysis with other approaches.

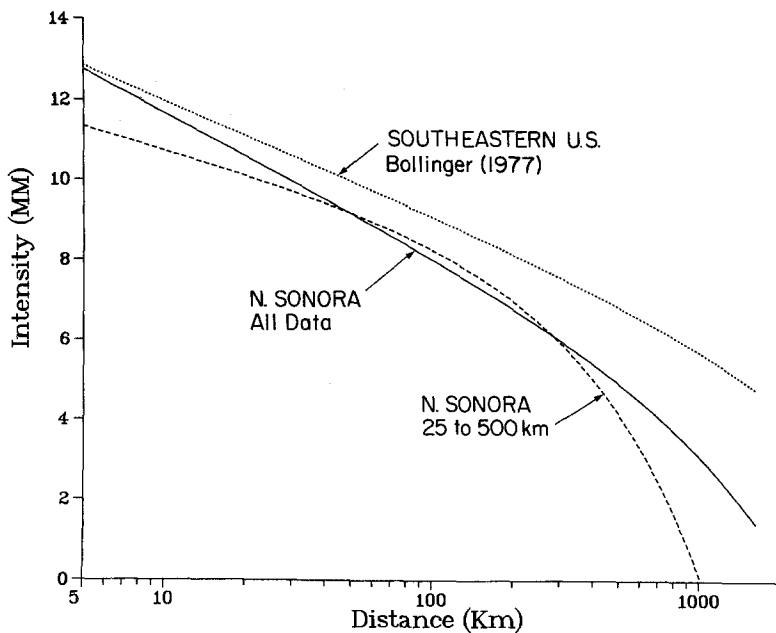


FIG. 5. Comparison of regression curves that are determined from individual intensity values.

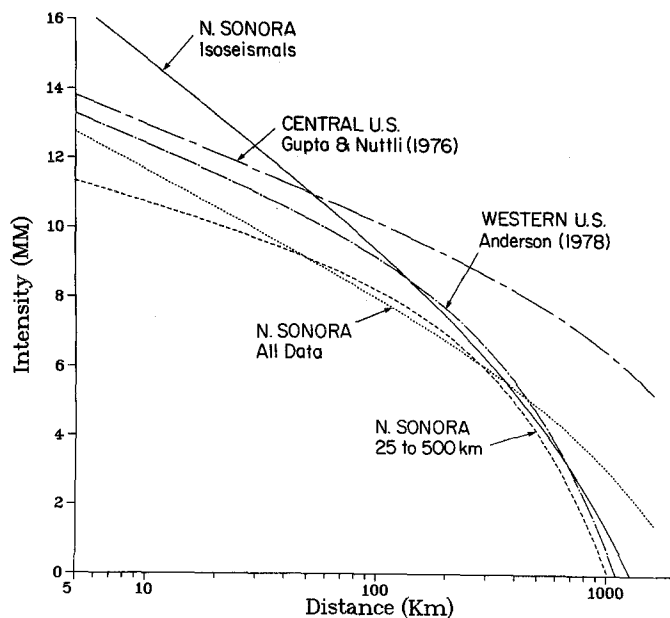


FIG. 6. Comparison of all northern Sonora regression curves with those for Central and Western United States.

The isoseismal and truncated curves for the northern Sonora data compare favorably with the Western United States curve for intensities less than or equal to MM X and MM IX, respectively. As noted above, the higher intensity portion of the isoseismal curve is unreliable. The regression using all data points has the same shape as the Central United States curve, but it is displaced below this by one to

two intensity units. Bollinger (1977) notes that the Gupta and Nuttli curve is about one intensity unit above his mean curve.

For approximately circular isoseismals, one would expect the regression curve to be greater than most data with intensity less than or equal to the value of the isoseismal. On the other hand, regression using individual intensity values should reflect the mean of those values at a given distance. Thus, one might expect the regression using individual points to be one to two units below the regression on

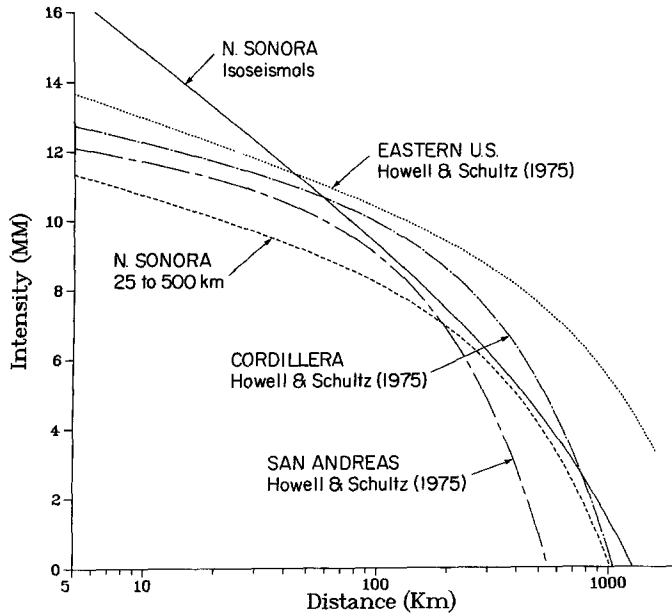


FIG. 7. Comparison of the isoseismal and the 25 to 500 km northern Sonora regression curves with the three regional curves of Howell and Schultz (1975).

TABLE 2
AREAS OF ISOSEISMALS AND AVERAGE RADII

MM Intensity	Area (km ²)	Average Radius (km)
XI	8,000	50
IX	48,000	124
VIII	91,000	170
VII	200,000	252
V	480,000	391
III	1,700,000	737

isoseismals depending on the scatter in the data as measured by σ_I in Table 1. The isoseismal curve for the 1887 earthquake follows this pattern from the highest intensities to MM VI; however the asymmetry of the intensity data at lower intensities brings the “all data” curve above the isoseismal curve.

Howell and Schultz (1975) compute regression curves for an Eastern United States set of five earthquakes and Cordilleran and San Andreas sets each of 10 events (Figure 7). The latter two sets are together comparable to the Western United States suite of earthquakes used by Anderson (1978). Howell and Schultz

determine average isoseismals using the same technique as used in Figure 4. The isoseismal curve has a different shape than those of Howell and Schultz, which may partly be a result of the low attenuation for the MM III isoseismal of the northern Sonora data. The curve for the truncated data set has the same shape as the Howell and Schultz curves, but lies significantly below theirs at the higher intensities. The curve for the truncated data set is similar to the Cordilleran curve for intensities less than MM IX.

These comparisons suggest that the attenuation coefficients for the region of the northern Sonora earthquake are essentially the same as those for other parts of Western United States, with the exception of paths along the Sierra Madre Occidental. For this region, attenuation coefficients similar to those for Central and Eastern United States should be used. The 1887 regression curve based on the truncated data set may be best for predicting the southern Basin and Range attenuation, whereas regression on all the data best reflects attenuation for paths along the Sierra Madre Occidental.

RELATIONSHIP BETWEEN INTENSITY AND SEISMIC MOMENT

Hanks *et al.* (1975) use the largest instrumentally recorded California earthquakes to establish an intensity-moment relationship, as a means of estimating the size of older earthquakes. Equation (2) represents their curve of best fit to the data.

$$\log(M_0) = 1.97 \log(A_{VI}) - 2.55 \quad (2)$$

where M_0 is the seismic moment, and A_{VI} is the area of the MM VI isoseismal in squared centimeters. They selected the MM VI isoseismal area as a standard, since this is usually well defined for a wide range of earthquakes. Unfortunately, this isoseismal is not clearly defined for the northern Sonora earthquake. Therefore, two areas were selected between those outlined by the MM V and VII isoseismals (Table 2) to evaluate the applicability of equation (2) to the 1887 study area. For an area of 3×10^{15} cm², a moment of 8.7×10^{27} dyne-cm is calculated and for an area of 4×10^{15} cm² the moment is 1.5×10^{28} dyne-cm². Both of these are significantly higher than the moment of 1.27×10^{27} dyne-cm calculated by Natali and Sbar (1982). We conclude that the Hanks *et al.* area-moment relationship is based on a region of higher attenuation for the MM VI isoseismal than exists in the study area. Figure 7 indicates that the average MM VI isoseismal plots about 100 km farther from the epicenter for the 1887 earthquake than for the San Andreas region. Similar data sets were used by both Howell and Schultz for the San Andreas zone and Hanks *et al.* for the moment-area relationship. Both comparisons indicate lower attenuation for the 1887 earthquake region than for the San Andreas region.

IMPLICATIONS FOR SEISMIC HAZARD

Analyses to date of the northern Sonora earthquake of 1887 provide valuable baseline information for considering the largest possible earthquake likely to occur in the area including southwestern New Mexico, southeastern Arizona and north-eastern Sonora. The intensity studies in particular indicate the impact an earthquake of this size had on the society and structures of the Southwest in 1887. It is important to consider the effect of a similar shock on current or future societies in this area. Although the likelihood of the Pitaycachi fault producing the next major earthquake is lower than that for adjacent faults, simply because it recently failed,

it is useful to consider a repeat of this shock as an initial step in the evaluation of earthquake hazard.

Near the epicenter, liquefaction effects caused significant ground failure leading to collapse of buildings and other structures. In part the liquefaction was caused by a shallow water table in the valleys surrounding the epicenter. Although the water table has been drawn down significantly in the active farming areas of Arizona and near the major cities, it is probably still quite shallow in the valleys that experienced liquefaction in 1887. Since most of the transportation routes, utilities, population centers, and other services are located in the valleys, considerable damage would be expected to these facilities and networks as a consequence of liquefaction. Landslides or rockfalls would be expected to recur along most of the mountain fronts characteristic of the Basin and Range morphology. Again some of the cities, roads, and other service lines run along the base of these mountains and damage due to this secondary effect will be of concern. Tucson, in particular, is experiencing rapid development into the foothills of the Santa Catalina and Tucson Mountains. Major cities such as Tucson and Hermosillo both experienced an intensity of MM VII in 1887. In both of these cities, single family housing is constructed of unreinforced masonry—one of the weakest construction materials for earthquake resistance. One would expect at least moderate damage in these structures. In much of Arizona, major structures are designed for zone 2 earthquake risk (Algermissen, 1969), and may thus sustain little damage at and less than the MM VII stage.

Locating the potential epicenter further to the north along the tectonically active zone of Pearthree *et al.* (1983) would bring it closer to Tucson and Phoenix increasing the impact on those cities. Moving it to the south would increase the impact on Hermosillo. The recurrence interval for an earthquake of approximately the size of the northern Sonora event is about 10^5 yr on a single fault (Bull *et al.*, 1981; Pearthree *et al.*, 1983). A number of faults have been mapped in the region around the 1887 epicenter, but no estimate of the recurrence interval for the entire zone has yet been made.

CONCLUSIONS

The intensity assignments of the northern Sonora earthquake have been contoured indicating a rather symmetric pattern for most isoseismal contours, the higher intensity isoseismals are strongly influenced by local basins and ranges, while the lowest intensity isoseismal is greatly extended along the structure of the Sierra Madre Occidental to the southeast and compressed at the Colorado Plateau-southern Basin and Range boundary to the north. A regression analysis of all the individual intensity values produced a curve similar to that for the southeastern United States, but indicates a higher attenuation. The northern Sonora curve also demonstrates lower attenuation for lower intensity levels than curves for the Western United States and Cordillera. A separate analysis used data only between 25 and 500 km from the epicenter to eliminate the effects of the fault itself and the low attenuation along the Sierra Madre Occidental. This regression yielded attenuation quite similar to that of the Western United States taken as a whole and the separate Cordillera analysis. Higher attenuation exists in the San Andreas region taken by itself than for the 1887 earthquake. Regression using the average radii of isoseismals produces results similar to the curve for individual data points between 25 to 500 km for data less than MM IX.

A relationship between seismic moment and the area circumscribed by the MM VI isoseismal derived from the San Andreas region (Hanks *et al.*, 1975) was tested

against the 1887 data. The predicted area was too small, suggesting lower attenuation in the study area than in the San Andreas region. The impact of an earthquake of this size on the Southwest would be disastrous. Further work is needed to establish the probability of damage due to earthquakes, so an informed decision can be made about appropriate building codes and levels of preparedness.

ACKNOWLEDGMENTS

This research was supported by National Science Foundation Grant EAR 82-12538, U.S. Geological Survey Contract 14-08-0001-18396, Nuclear Regulatory Commission Contract 04-79-212, and the Arizona Bureau of Geology and Mineral Technology. Critical review by Dan J. Cash of Los Alamos National Laboratory, John G. Anderson of IGPP at Scripps Institution of Oceanography, and Otto Nuttli of St. Louis University is deeply appreciated.

REFERENCES

- Algermissen, S. T. (1969). Seismic risk map of the United States, *Proc. of the Fourth World Conf. on Earthquake Engineering, Santiago, Chile* **1**, 14–27.
- Anderson, J. G. (1978). On the attenuation of modified Mercalli intensity with distance in the United States, *Bull. Seism. Soc. Am.* **68**, 1147–1179.
- Bollinger, G. A. (1977). Reinterpretation of the intensity data for the 1886 Charleston, South Carolina, earthquake, in *Studies related to the Charleston, South Carolina, Earthquake of (1886)—A preliminary report*, U.S. Geol. Surv. Profess. Paper 1028-B, 32 pp.
- Braze, R. J. (1979). Reevaluation of modified Mercalli intensity scale for earthquakes using distance as a determinant, *Bull. Seism. Soc. Am.* **69**, 911–924.
- Bull, W. B., S. S. Calvo, P. A. Pearthree, and J. Quade (1981). Frequencies and magnitudes of surface rupture along the Pitaycachi fault, northeastern Sonora, Mexico, *Geol. Soc. Am. Abstracts with Programs* **13**, 47.
- de Cserna, A., B. C. Hezon, and D. Saldana (1961). Tectonic map of Mexico, Geological Society of America Publication.
- DuBois, S. M. and A. W. Smith (1980). The 1887 earthquake in San Bernardino Valley, Sonora: Historic accounts and intensity patterns in Arizona, *Ariz. Bur. Geol. and Min. Tech., Special Paper No. 3*, Tucson, Arizona, 112 pp.
- Gupta, I. N. and O. W. Nuttli (1976). Spatial attenuation of intensities for central U.S. earthquakes, *Bull. Seism. Soc. Am.* **66**, 743–751.
- Hanks, T. C. and H. Kanamori (1979). A moment magnitude scale, *J. Geophys. Res.* **85**, 2348–2350.
- Hanks, T. C., J. A. Hileman, and W. Thatcher (1975). Seismic moments of the larger earthquakes of the southern California region, *Bull. Geol. Soc. Am.* **86**, 1131–1139.
- Herd, D. G. and C. R. McMasters (1982). Surface faulting in the Sonora, Mexico earthquake of 1887, *Geol. Soc. Am. Abstracts with Programs* **14**, 172.
- Howell, B. J., Jr. and T. R. Schultz (1975). Attenuation of Modified Mercalli intensity with distance from the epicenter, *Bull. Seism. Soc. Am.* **65**, 651–665.
- Natali, S. G. and M. L. Sbar (1982). Seismicity in the epicentral region of the 1887 northeastern Sonoran earthquake, Mexico, *Bull. Seism. Soc. Am.* **72**, 181–196.
- Nuttli, O. W. (1973). The Mississippi Valley earthquakes of 1811 and 1812: intensities, ground motion and magnitudes, *Bull. Seism. Soc. Am.* **63**, 227–248.
- Pearthree, P. A., C. M. Menges, and L. Mayer (1983). The distribution, recurrence and possible tectonic implications of late Quaternary faulting in Arizona, in Final Report, U.S. Geological Survey Contract No. 14-08-0001-19861.
- Richter, C. F. (1958). *Elementary Seismology*, W. H. Freeman and Co., San Francisco, California, 768 p.
- Seager, W. and P. Morgan (1979). Rio Grande rift in southern New Mexico, west Texas and northern Chihuahua, in *Rio Grande Rift: Tectonics and Magmatism*, R. Reicker, Editor, Am. Geophys. Union, Washington, D.C., 87–106.

DEPARTMENT OF GEOSCIENCES
UNIVERSITY OF ARIZONA
TUCSON, ARIZONA 85721 (M.L.S.)

DUBOIS GEOTECHNICAL SERVICES, INC.
1835 NORTH STEVENS STREET
RHINELANDER, WISCONSIN 54501 (S.M.D.)

APPENDIX

Site	Intensity (mm)	North Latitude	West Longitude	Distance (km)	Azimuth
Pitaycachi	12.0	31.01	109.12	5.04	48.71
Penasquito	12.0	30.92	109.13	9.17	165.25
La Cabellera	12.0	30.83	109.13	16.86	170.41
San Bernardin Mt.	7.0	31.03	109.33	17.53	280.98
Los Embudos Canyon	12.0	31.13	109.22	17.60	340.89
Batepito River Valley	10.5	30.82	109.20	18.16	192.39
Cuchuverachi	10.5	31.15	109.17	18.89	355.93
Sierra Los Embud	7.0	31.16	109.07	19.32	23.34
Cajon Del Alamo	12.0	30.80	109.27	19.96	182.18
Batepito Ranch	10.0	30.82	109.10	20.50	166.66
San Bernardino River Valley	10.5	30.80	109.18	22.34	187.10
Teras Mt.	10.5	30.75	109.17	25.51	182.21
Cinco De Mayo	12.0	30.73	109.13	27.87	173.87
Fronteras River Valley	10.0	31.12	109.42	29.98	297.38
Fronteras	11.0	30.93	109.52	34.83	260.94
Guadalupe Gorge	11.0	31.28	109.28	35.17	341.03
Guadalupe	12.0	31.29	109.27	35.94	343.01
Cuchuta	9.0	30.82	109.50	37.04	241.48
San Bernardino River Valley	10.0	31.33	109.27	40.19	344.87
Sierra Cabullona	7.0	31.08	109.58	41.99	282.30
Cabullona	5.0	31.16	109.56	42.95	294.49
Sierra Turicachi	7.0	30.73	109.53	47.07	230.62
Agua Preita Valley	9.0	31.25	109.55	47.75	308.91
Carretas Range	7.0	30.65	108.78	51.59	135.06
San Miguel	8.0	30.52	108.97	54.13	160.31
Penuelas Springs	7.0	30.80	108.60	57.13	110.30
Sierra Pinito	7.0	30.55	109.53	61.72	216.19
Bavispe	11.5	30.40	108.83	71.64	153.72
Callejon	11.5	30.30	108.83	83.00	158.36
Bavispe River Valley	11.5	30.50	108.83	63.00	150.99
Magallanes Mt.	7.0	31.10	109.93	74.69	280.46
Nacozari	8.5	30.40	109.65	79.59	216.26
Baceras	8.5	30.30	108.83	81.73	157.15
Bacoachi	10.0	30.68	109.93	82.60	244.77
San Jose Mt.	7.5	31.27	109.98	84.55	292.56
Nacozari Range	8.5	30.33	109.67	87.06	214.29
Bisbee	7.5	31.44	109.92	88.57	305.34
Rucker Canyon	7.0	31.77	109.30	88.58	351.36
Huachinera Valley	7.0	30.27	108.75	89.53	154.54
Chiricahua Mt.	8.0	31.80	109.30	89.82	350.91
Mule Pass	6.0	31.45	109.95	91.54	304.89
Abbot's Range	10.0	31.53	109.88	91.75	311.82
Janos	9.5	30.90	108.17	95.01	95.10
Huachinera	7.0	30.15	108.92	96.75	166.76
Oputo	10.0	30.05	109.33	104.35	189.04
Huachinera Valley	7.0	30.05	108.83	107.83	162.83
Diez	7.0	31.15	108.00	112.29	80.04
Riggs' Ranch	6.0	32.00	109.40	113.36	347.98
Corr. Mining Co.	7.5	30.72	108.00	114.62	104.26
Miller Canyon	7.0	31.40	110.27	115.57	294.04
Huachuca Reservoir	9.0	31.68	110.10	117.69	310.07
Tombstone	7.5	31.71	110.07	118.51	313.30
Charleston	10.0	31.62	110.17	119.48	306.68
Carr Canyon	7.0	31.43	110.30	119.52	294.96
Gusabas	9.0	29.90	109.30	120.45	186.47
Arizpe	10.0	30.33	110.17	120.65	233.60
Cumpas	8.5	30.03	109.80	121.89	210.42

APPENDIX—Continued

Site	Intensity (mm)	North Latitude	West Longitude	Distance (km)	Azimuth
Fairbank	9.0	31.72	110.19	127.79	310.20
Cochise's Strong	7.0	31.90	110.00	129.52	322.16
Bear Spring	7.0	32.13	109.42	129.85	349.11
Huachuca Mt.	10.0	31.48	110.40	130.48	295.45
Ft. Huachuca	7.0	31.63	110.33	132.64	303.20
Babocomari	7.0	31.65	110.33	133.85	304.00
Dragoon Mt.	8.0	31.95	110.00	133.91	323.63
Casas Grandes	7.0	30.37	107.95	134.20	119.94
Sierra Azul	7.0	30.77	110.57	138.12	259.73
Bloxton's Range	8.5	31.60	110.42	138.24	300.13
Bacadehuachi	8.5	29.73	109.17	138.53	180.43
Granados	9.5	29.73	109.32	138.53	180.43
Badehuachi	9.0	29.85	109.75	139.88	204.49
Washington Camp	6.5	31.42	110.55	141.14	290.57
San Simon	7.0	32.27	109.23	143.15	357.36
St. David	9.5	31.90	110.22	143.35	315.62
Mustang Hills	7.5	31.67	110.47	146.25	301.87
Delicas	8.0	29.98	110.18	147.88	221.72
Montezuma	9.5	29.72	109.68	148.32	199.83
Elgin	6.5	31.66	110.52	149.78	300.57
Whetstone Mt.	8.5	31.78	110.45	151.38	306.19
Bowie	8.0	32.32	109.49	151.81	348.18
Chivato Mt.	7.0	30.95	110.75	151.91	269.15
Benson	8.0	31.96	110.30	153.41	315.38
Box Canyon	8.0	31.55	110.63	153.57	294.67
Willcox	7.5	32.25	109.84	154.86	335.56
Harshaw	6.5	31.47	110.70	156.44	290.71
Tres Alamos	10.0	32.05	110.28	159.32	318.40
Patagonia Mt.	7.0	31.43	110.75	159.50	288.63
Guerrero	7.0	30.47	110.70	159.61	248.80
Crittenden	6.0	31.65	110.70	164.31	297.27
Totalwreck	7.0	31.90	110.60	170.68	307.06
Tepic	10.0	29.47	109.43	171.69	189.11
Empire Ranch	9.0	31.90	110.63	172.44	305.73
Ash Canyon	7.0	31.53	110.87	174.00	290.18
Nogales	6.5	31.34	110.94	174.31	283.69
Galeana	8.0	30.12	107.63	175.00	122.61
Magdalena	7.0	30.63	110.95	175.60	257.69
Pantano	7.5	32.00	110.58	176.01	310.34
Davidson's Canyon	7.0	31.95	110.65	177.78	307.60
Santa Rita Mt.	7.0	31.68	110.85	178.55	296.19
Calabasis	7.0	31.47	110.98	181.68	287.86
Santa Cruz River Valley	7.0	31.50	111.00	184.49	288.68
Deming	7.5	32.26	107.76	194.35	42.74
Graham Mt.	7.0	32.67	109.92	200.68	339.19
Whitewater Canyon	8.0	32.77	109.58	202.38	348.79
Ft. Thomas	5.0	33.03	109.95	207.69	347.76
Solomonville	7.0	32.81	109.63	207.69	347.76
Ures	7.5	29.43	110.40	209.17	215.11
Oro Blanco	6.0	31.48	111.28	209.41	285.89
Sahuaripa	8.5	29.05	109.23	213.98	181.86
Silver City	7.5	32.77	108.28	215.19	22.53
Alamos	3.0	29.22	110.13	216.28	205.85
Arivaca	5.0	31.58	111.33	217.04	288.40
Santa Catalinas	8.0	32.42	110.75	219.53	317.06
Tucson	7.5	32.22	110.97	219.97	309.14
Nocori	6.5	29.07	110.05	230.81	202.31

APPENDIX—Continued

Site	Intensity (mm)	North Latitude	West Longitude	Distance (km)	Azimuth
Oracle	7.5	32.61	110.76	235.80	320.44
Mammoth	7.0	32.72	110.64	238.37	324.40
Dripping Springs	5.0	33.03	110.77	239.21	342.03
Altar	7.0	30.72	111.73	247.45	263.97
Kingston	5.0	32.92	107.70	253.15	32.40
Dudleyville	4.5	32.91	110.70	257.48	325.72
Mesilla	6.0	32.27	106.80	265.63	56.82
El Paso	7.5	31.76	106.48	269.17	70.57
Coyote Mt.	7.0	31.97	111.75	269.43	294.70
Las Cruces	6.5	32.31	106.78	269.59	56.23
Hermisillo	7.0	29.07	110.97	274.34	219.97
San Elizaro	3.0	31.59	106.27	283.31	75.45
San Carlos Reservoir	7.0	33.30	110.50	285.01	333.82
Organ	4.5	32.43	106.60	289.00	56.07
Torres Station	7.0	28.77	110.78	290.60	212.98
San Carlos	6.0	33.36	110.78	304.88	330.36
Globe	6.5	33.40	110.78	308.71	330.77
Pinal	6.0	33.30	111.08	314.56	325.35
Picket Post Mt.	7.0	33.27	111.15	315.75	324.04
Gila Company	7.0	33.50	110.80	317.78	331.15
Ft. Apache	7.5	33.78	109.98	319.88	346.26
San Francisco	3.0	30.80	112.57	326.57	267.37
Maricopa	3.0	33.06	112.05	357.31	310.94
Sierra Blanca	3.0	31.18	105.36	363.20	85.53
San Marcial	6.5	33.70	106.98	364.73	33.66
Baroyeca	3.0	27.65	109.50	370.44	185.20
Salt River	6.5	33.38	112.00	377.47	315.56
Ft. McDowell	6.5	33.63	111.68	377.63	321.74
Guaymas	4.0	27.93	110.90	377.72	206.96
Cape Haro	6.5	27.90	110.92	381.57	207.01
Phoenix	6.0	33.45	112.07	387.55	315.72
Chihuahua City	5.0	28.63	106.08	395.46	130.41
Gila Bend	3.0	32.95	112.72	401.09	303.91
Gila Crossing	5.0	33.41	112.34	402.22	312.46
Gulf of California	3.0	28.00	112.00	432.19	220.44
Sabinal	8.5	34.49	106.80	445.00	29.02
Rosales	5.0	28.20	105.55	465.92	130.48
Prescott	2.0	34.55	112.47	502.78	322.80
Ft. Davis	3.0	30.59	103.90	505.17	93.56
Santa Rosalia	4.0	27.35	112.31	508.00	218.01
Albuquerque	6.0	35.08	106.65	511.48	26.61
Colo & Gila Junction	3.0	32.53	114.55	538.64	290.00
Yuma	4.5	32.72	114.72	560.30	291.58
Jiminez	3.0	27.13	104.92	593.47	134.90
Santa Fe	3.0	35.68	105.94	610.60	332.57
Macorita	3.0	25.52	107.97	615.99	168.79
Las Vegas	2.0	35.60	105.22	627.68	34.60
Bolson De Mapimi	3.0	27.50	103.50	672.00	123.83
La Mesa	6.5	32.74	101.96	706.90	72.30
Ciudad Lerdo	5.0	25.53	103.53	818.88	136.35
Durango	4.0	24.03	104.67	888.14	148.99
Mazatlan	3.0	23.22	106.42	901.23	161.82
Los Angeles	1.0	34.06	118.25	919.21	294.04
Zacatecas	3.0	22.78	102.75	1108.47	143.47
Guanajuato	2.0	21.02	101.25	1356.48	142.52
Toluca	3.0	19.30	99.65	1607.86	141.32
Mexico City	4.0	19.40	99.15	1629.26	139.56